Study of the Electrical Properties of Thin Silica Layers with a Single Plane of AgNPs Embedded Near the Surface

C. Rigoudy, Kremena Makasheva, C. Villeneuve-Faure, G. Teyssedre, Laurent Boudou

Study of the Electrical Properties of Thin Silica Layers with a Single Plane of AgNPs Embedded Near the Surface

C. Rigoudy, K. Makasheva, C. Villeneuve-Faure, G. Teyssedre and L. Boudou
LAPLACE, Université de Toulouse, CNRS, INPT, UPS, Toulouse, France

***Abstract*- The present work explores the effect of metal inclusions (silver nanoparticles, AgNPs) on the electrical mechanisms (charge injection, trapping and transport) responsible for dielectric charging in thin silica layers. It is shown that the presence of a plane of AgNPs embedded in a thin SiO_2 layer modifies the electrical conduction in the structure. When the AgNPs-plane is embedded near the SiO_2 surface, the structure behaviour at low electric field is non-ohmic and does not allow calculation of the classical volume conductivity. Instabilities in the behaviour of the structure are observed for high electric fields. They are most likely due to sequences of breakdown/self-healing phenomena that clearly appear for fields higher than 10^8 V/m.**

I. Introduction

All electrical and electronic devices require knowledge and control of the response of the dielectric materials, involved in their structures, under electrical stress. To accomplish this, an analysis of the electrical mechanisms (charge injection, trapping and transport) responsible for the dielectric charging phenomenon becomes indispensable. The dielectric charging phenomenon, *i.e.* the ability of dielectric materials to trap electrical charges, leads to modification of the local electric field. It causes changes in the electrical behavior of the device, and on a longer term a degradation of the dielectric properties of the materials under electrical stress [1, 2]. Although the electrostatic charging of thin dielectric layers lays down the principle of operation of various technological devices, like non-volatile memories [3] or electret based microphones [4], it is considered to be the main cause of electrostatic sticking in MicroElectroMechanical Systems (MEMS) [5] or for the appearance of Electrostatic Discharges (ESD) that lead to the damage of the electronic devices, especially in space environment, and thus shorten their lifetime [6].

A considerable progress on the study of the dielectric response under electrical stress and on many of the global electrical parameters of dielectrics (permittivity, losses, low field conductivity, space charge, *etc*.) was achieved since the beginning of application of nanocomposite dielectrics, or nanodielectrics, in the early 90s [7]. Improved performance of the dielectric materials has been demonstrated for dielectrics containing nanoparticles, either dispersed in the volume [8, 9] or embedded in a layered structure [10 – 12]. However, the fine description of the physical phenomena occurring in the dielectrics, in the presence of nanoparticles, is still incomplete. The latter is mainly due to the complexity conveyed to the dielectrics by the nanoparticles.

In this work we present a study on the changes of the electrical response of thin silica layers containing a single plane of silver nanoparticles (AgNPs) embedded near the dielectric surface. The aim is to complement the knowledge on charge injection, trapping and transport phenomena in thin dielectrics. Such approach allows us to achieve a better understanding of the nonlinear mechanisms induced by the presence of metallic inclusions in a dielectric layer. Working with a plane of AgNPs embedded in the vicinity of the dielectric surface, rather than with dispersed in the volume metallic nanoparticles, permits to reduce the complexity of the problem by reducing its dimensions, from 3D to 2D. Such AgNPs-nanocomposites can be successfully applied as charge barrier layers for charge injection in polyethylene used as insulator in High Voltage Direct Current-HVDC lines [12], in capacitors for energy storage [13], or to control the secondary electron emission phenomena in space applications [14]. Generally speaking, many electronic devices and applications are concerned by this fundamental study because of the stratified architectures of the dielectric layers in them. Among others, one can mention here different heterojunction devices for non-volatile memories [3], [15], including flexible non-volatile memory devices [16], highly-transparent metallic nanowire based electrodes [17], resistive switching devices [18], etc.

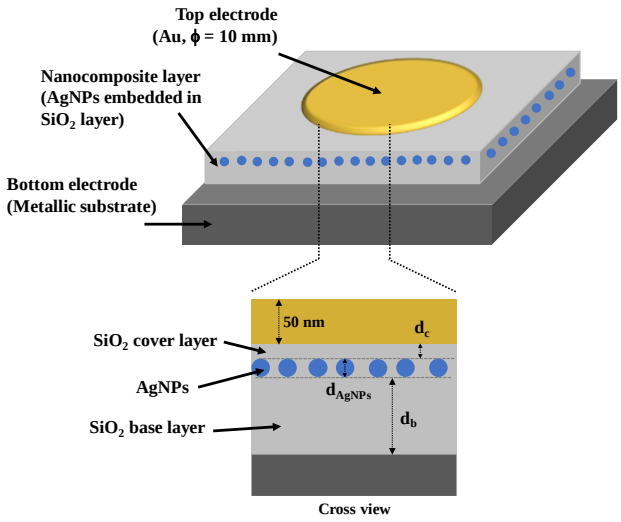

Fig. 1. Scheme of AgNPs nanostructure.

II. Sample Elaboration And Characterization Methods

The targeted nanocomposites (NCs) consist in a single plane of AgNPs embedded at a fixed distance beneath the surface of a SiO_2 layer deposited on metallic substrates (mirror polished stainless still with size 3.3 cm × 3.3 cm) and on intrinsic Si-substrates (Fig. 1). The use of metallic substrates is based on considerations related to electrical measurements. The stainless still substrates ensure good electrical contact on the back side of the structure for the charge current and breakdown measurements, while the Si-substrates are used for cross-section analyses by Transmission Electron Microscopy (TEM). For the electrical characterization a circular top Au-electrode (50 nm thick and 1 cm in diameter) was sputtered on the sample surface to complete the Metal-Insulator-Metal (MIM) structure.

A. Plasma process for sample elaboration

The AgNPs nanostructured thin dielectric layers have been elaborated in a plasma process combining in the same reactor sputtering of an Ag target and plasma polymerization [11, 19]. The plasma was sustained in argon gas at low gas pressure p = 5.3 Pa for the Ag-sputtering. The size and density of the obtained AgNPs were controlled by the injected in the plasma power and the sputtering time (t_s). The presented here samples are for injected power P = 80 W and t_s = 5 s. Using the same vector gas (argon), the precursors added in the plasma for the SiO_2 deposition were hexamethyldisiloxane (HMDSO, $C_6H_{18}Si_2O$) and O_2. The SiO_2-base and the cover layers were deposited in the plasma sustained by P = 120 W, at total pressure of p_{tot} = 7.9 Pa. Details on the reactor geometry, the plasma behaviour and the process parameters are given in [11, 19]. Table I summarizes the parameters of the tested samples. For correspondence with the MIM structures, see Fig. 1.

TABLE I. Samples For Conductivity Measurements And *Samples For Breakdown And Self-Healing Tests

Sample	SiO_2 base thickness d_b (nm)	AgNPs diameter d_{AgNPs} (nm)	Cover layer thickness d_c (nm)
107 nm-SiO_2	107	/	/
NC1	112.1	18	6.9
NC2	104.6	18	9.1
NC3	97.8	18	55.5
***50 nm-SiO_2**	50	/	/
***NC4**	175	18	8

B. Structural and electrical characterization methods

The different values, reported in Table I, correspond to measurements of the nanocomposites made by spectroscopic ellipsometry for the SiO_2 layers thicknesses and composition and by TEM analyses for the size and density of the AgNPs. Information on the surface topography of the elaborated nanocomposites was obtained by AFM measurements, using a Multimode 8 Bruker apparatus.

The electrical properties of the AgNPs nanocomposites have been studied through measurements of the polarization currents under DC voltage application in the range from 0.1 V to 100 V, corresponding to electric fields varying from 10^6 V/m to 8×10^8 V/m approximatively. The study of polarization currents was performed through a protocol of successive and increasing voltages. Each voltage step lasted for 1000 s and was followed by a depolarization time at 0 V during 1000 s. The voltage was applied between the metallic substrate connected to the electrometer and the upper Au-electrode connected to the voltage supply.

Breakdown and self-healing phenomena were studied using the voltage protocol described previously, except for the polarization and depolarization times lowered to 15 s for each step. The sample surface was observed under an optical microscope and the analysis was performed on video recordings, taken during the voltage application.

III. Results and Discussion

A. AgNPs nanocomposites: quality of the dielectric layer and control of the distance of the AgNPs plane to the surface

Direct observation by TEM in a cross-section view allows characterization of the elaborated nanostructures: thickness of base SiO_2 layer and cover SiO_2 layer and planarity of the sample surface. In addition, a paired analysis with plane view TEM images gives the size and distribution of AgNPs in the plane. As an example, Fig. 2a presents the cross-section view of a nanostructure with targeted layer thicknesses of d_b = 190 nm and d_c = 10 nm. The extracted thicknesses of the base SiO_2 layer is of 182 nm and that of the SiO_2 cover layer is of 9.5 nm. This result confirms the importance of fine control during the plasma elaboration process and validates the applied methods permitting strict control of alignment of the AgNPs at a given nanometric distance beneath the SiO_2 surface. Moreover, the obtained results are in accordance with those extracted from spectroscopic ellipsometry and in agreement with previous works for the same plasma parameters [11, 19].

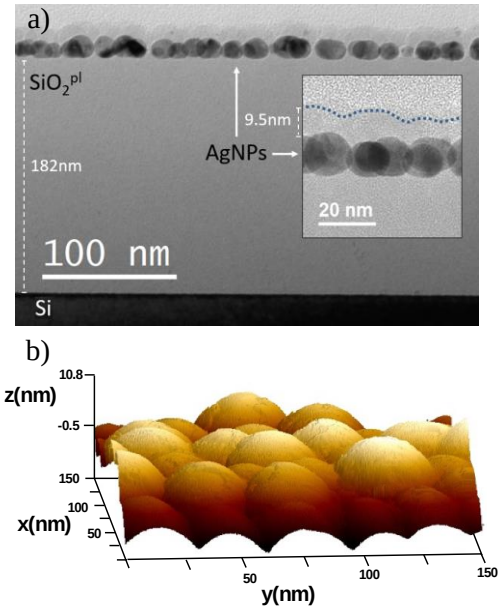

Fig. 2. (a) Cross-section view TEM image of the SiO_2/AgNPs sample. Insert: enlargement of the near surface part; (b) AFM topography of the SiO_2/AgNPs sample with a 5 nm cover layer thickness.

AFM surface topography of an AgNPs-based NC with only a 5 nm thick cover layer is presented Fig. 2b. It emphasizes the irregularity of the surface imposed by the conformity of the SiO_2 cover layer. Since the plasma deposited thin layers are conformal to the surface one can notice the waviness of the dielectric surface due to the AgNPs-shape fitting by the SiO_2 cover layer. The point is that for large AgNPs and very thin SiO_2 cover layers the formed dips might be of up to 10 nm in size in between the AgNPs and may give rise to quite sharp metallic "tips" when the top Au-electrode is sputtered. The so-created metallic tips would lead to a strong enhancement of the electric field at that points, called hereafter "hot points", and to a preferential local injection of electrical charges, which shall be accounted for in the analysis of the electrical response of the NCs. However, when increasing the SiO_2 cover layer thickness, the surface waviness is rapidly smoothed, as can be seen in the insert of Fig. 2a, for which the SiO_2 cover layer is of 9.5 nm. The created irregularities are then reduced to only 2 – 3 nm.

B. Conductivity of the AgNPs containing MIM structures

Fig. 3. represents the current density (J) versus the applied electric field (E) for all samples, reported in Table I. The electric field values reported in the x-axis are calculated here considering a plane to plane classical configuration. Local field enhancement, due to the presence of AgNPs-plane into the dielectric layer [20] or to metallic tips at the interface between the Au-top electrode and the SiO_2 cover layer, is not taken into account for the $J(E)$ plots. Open symbols represent instabilities in the measured current observed in the case of AgNPs plane positioned near the surface (6.9 and 9.1 nm).

1. Conductivity at low electric field

Fig. 3 shows that the current density for the nanocomposites is higher compared to the SiO_2 reference sample, and that it strongly depends on the distance of AgNPs plane from the surface. The recorded current density in the low field region ($< 10^7$ V/m) is at least 4 orders of magnitude higher when the AgNPs plane is near the surface (6.9 and 9.1 nm for samples NC1 and NC2, respectively). However, in this field region, the $J(E)$ characteristics show a non-ohmic behavior (slope higher than unity in a log-log plot) and do not allow calculation of the classical volume conductivity. When the AgNPs plane is embedded far from the surface ($d_c = 55.5$ nm), an ohmic behaviour is observed and the conductivity of the nanocomposite decreases to get closer to the conductivity of the SiO_2 reference sample estimated to 1.2×10^{-16} S/m.

2. Nonlinear phenomena observed at high electric field

In the high electric field region, the conductivity is not constant with the field. It starts increasing with the electric field, for strengths higher than 2×10^8 and 3×10^7 V/m, for the 107 nm-SiO_2 and NC3 samples, respectively. For sample NC1 and NC2 no threshold field is observed. Moreover, non-linear phenomena occur. Current instabilities are observed for NC1 and NC2 samples, for which the AgNPs-plane is closely situated to the surface, and are probably linked to breakdown followed by self-healing phenomena, as discussed in section C.

The shape of the $J(E)$ plot for NC3 sample (AgNPs-plane embedded deeper in the SiO_2, at 55 nm from the surface) consists in successive linear regions with slopes very similar to those described in the limits of the Space Charge Limited Conduction (SCLC) theory. This behaviour is identical with the case of nanocomposites, with low volume fractions of randomly dispersed in a dielectric matrix metallic NPs, for which the conduction is controlled by both the ability of NPs to act as deep trapping centers and the dielectric properties of the dielectric matrix itself in terms of traps density and their energy level distribution, in the frame of the SCLC mechanism [21]. However, complementary work, including space charge measurements at local scale, is needed to confirm this point.

In the case of very thin cover layer (5 nm or less), local field enhancement due to the topography of interface between the SiO_2 cover layer and the Au-electrode is likely. The measured current is then higher than expected. As extracted from Fig. 2b, the most pronounced dip in the surface topography creates a metallic tip with curvature radius 10 nm after deposition of the top Au-electrode. Thus, the electric field at such hot point is locally enhanced by a factor of 6.5 when compared to the electric field in plane-to-plane configuration. Accordingly, a stronger charge injection occurs locally at the hot points and the measured integral current of the MIM structure is higher.

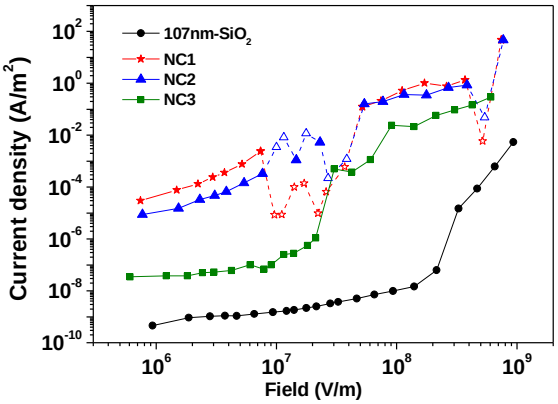

Fig 3. Current density vs. electric field of thin SiO_2 layer (black circles) and the SiO_2/AgNPs nanostructures. The open symbols represent instabilities in the current density measurements.

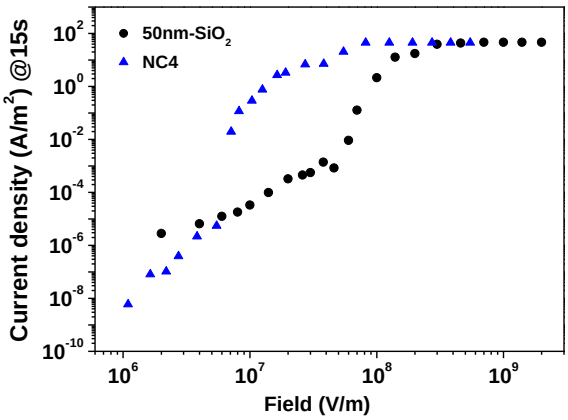

Fig. 4. Current density recorded after 15 s of voltage application for a SiO_2 reference sample and the AgNPs-based nanocomposite NC4.

C. *Breakdown and self-healing phenomena under DC voltage*

The term of self-healing or clearing phenomena is used for a MIM structure to qualify its ability to self-repair and recover its capacitor behavior after a breakdown [22]. A consequence of the self-healing phenomena is a decrease of the effective area of the metallic electrode and then a decrease of the capacitance. In order to study these phenomena for the developed nanostructures, a reference sample (50 nm thick SiO_2) and a nanocomposite sample (NC4) were submitted to the DC voltage protocol already described in section II.B.

Fig. 4 represents the current density recorded 15 seconds after the voltage application as a function of the applied electric field for the 50 nm-SiO_2 reference sample and the nanocomposite NC4. In the presence of AgNPs plane and for very low field (lower than 5×10^6 V/m) the recorded current is lower compared to the bare SiO_2 sample. In the field range 10^7 - 10^8 V/m the current recorded for NC4 is several decades higher compared to the bare SiO_2 sample, in good correlation with the results obtained for long time measurements (Fig. 3). For electric field around 10^8 V/m and higher, the current is maximum and limited by the voltage supply; breakdowns followed by self-healing phenomena are clearly visible on the surface of the top-electrode. Most likely, the breakdowns/self-healing phenomena occur even for lower fields, in the 10^7 - 10^8 V/m range, but remain difficult to observe due to the limited resolution of the optical system.

Fig. 5 shows successive pictures extracted from a video recording of the sample surface. At time T_0 no visible breakdown can be identified on the entire Au-top electrode. At time T_1 a light emitting breakdown (within the red circle) at a specific point of the surface appears. It can be due to defect of the dielectric layer or to a field enhancement at a specific "hot point". This first breakdown is situated at several mm from the edge of the Au-electrode. At time T_2 the thin Au-electrode has been evaporated around the first breakdown point; the corresponding conducting channel (breakdown channel) is disconnected from the electrode and the insulation is recovered and new breakdowns can appear. At time T_3 the same behavior that consists in a succession of breakdown/self-healing/new breakdown events is observed. These phenomena are observed for both samples. However, in presence of the AgNPs plane they appear at lower electric field.

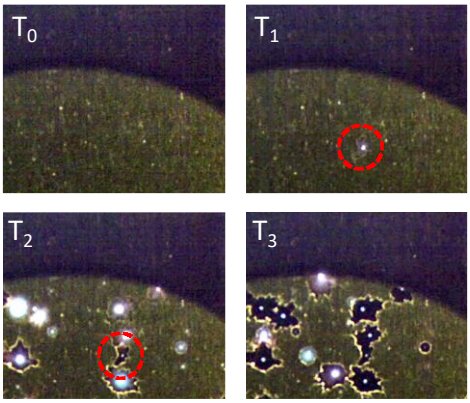

Fig. 5. Illustration of self-healing phenomena on the surface of NC4 sample: applied DC voltage 100 V. Top view pictures (4.0 × 3.4 mm^2) extracted from recorded video of the surface. T_0 before voltage application. T_1 = 33 ms, T_2 = 66 ms and T_3 = 100 ms after voltage application.

IV. Conclusion

This work is a demonstration of the capability of AgNPs to locally modify the electrical properties of dielectric materials under electric stress. The addition of AgNPs in a thin silica layer allows for efficient modification of the conduction of the MIM structure, depending on the distance of the AgNPs-plane to the dielectric surface.

Acknowledgment

Research supported by the program IDEX ATS 2015 of the Université de Toulouse under project SEPHIR (2016-066-CIF-D-DRVD). The authors acknowledge support from the UAR Raymond Castaing of Université de Toulouse and thank Dr. A. Pugliara and Mr. L. Weingarten for the TEM observations.

References

[1] C. A. Rezende, *et al.*, "Detection of charge distributions in insulator surfaces," *J. Phys. Condens. Matter*, vol. 21, p. 263002, 2009.

[2] C. Laurent, G. Teyssedre, S. Le Roy, and F. Baudoin, "Charge dynamics and its energetic features in polymeric materials," *IEEE Trans. Dielectr. Electr. Insul.*, vol. 20, pp. 357–381, 2013.

[3] P. Dimitrakis, I. Valov, and S. Tappertzhofen, *Metal oxides for non-volatile memory: materials, technology and applications*. Elsevier, 2022.

[4] G. M. Sessler, Ed., *Electrets*, vol. 33. Berlin, Heidelberg: Springer Berlin Heidelberg, 1987.

[5] G. M. Rebeiz, *RF MEMS: theory, design, and technology*. Hoboken, NJ: J. Wiley, 2003.

[6] N. Balcon, *et al.*, "Secondary Electron Emission on Space Materials: Evaluation of the Total Secondary Electron Yield From Surface Potential Measurements," *IEEE Trans. Plasma Sci.*, vol. 40, pp. 282–290, 2012.

[7] T. J. Lewis, "Nanometric dielectrics," *IEEE Trans. Dielectr. Electr. Insul.*, vol. 1, pp. 812–825, 1994.

[8] T. Tanaka and T. Imai, "Advances in nanodielectric materials over the past 50 years," *IEEE Electr. Insul. Mag.*, vol. 29, pp. 10–23, 2013.

[9] S. Diaham, "Modulation of the dielectric breakdown strength in polyimide nanocomposites by deep traps tailoring in interphase regions," *IEEE Trans. Dielectr. Electr. Insul.*, vol. 26, pp. 247–252, 2019.

[10] N. Zhao, *et al.*, "Effects of LDPE/nanofilled LDPE interface on space charge formation," in *2013 IEEE ICSD*, Bologna, Italy, pp. 944–947, 2013.

[11] K. Makasheva *et al.*, "Dielectric Engineering of Nanostructured Layers to Control the Transport of Injected Charges in Thin Dielectrics," *IEEE Trans. Nanotechnol.*, vol. 15, pp. 839–848, 2016.

[12] L. Milliere, *et al.*, "Silver nanoparticles as a key feature of a plasma polymer composite layer in mitigation of charge injection into polyethylene under dc stress," *J. Phys. Appl. Phys.*, vol. 49, p. 015304, 2016.

[13] R. Wen, *et al.*, "Nanocomposite Capacitors with Significantly Enhanced Energy Density and Breakdown Strength Utilizing a Small Loading of Monolayer Titania," *Adv. Mater. Interfaces*, vol. 5, p. 1701088, 2018.

[14] C. Rigoudy, K. Makasheva, M. Belhaj, S. Dadouch, G. Teyssedre, and L. Boudou, "Atypical secondary electron emission yield curves of very thin SiO_2 layers: Experiments and modeling," *J. Appl. Phys.*, vol. 130, p. 135305, 2021.

[15] Z. Çaldıran, *et al.*, "SCLC in the graphene oxide–Fe_3O_4 nanocomposites/n-Si heterojunctions," *J. Alloys Compd.*, vol. 631, pp. 261–265, 2015.

[16] S. Sung and T. W. Kim, "Flexible nonvolatile memory devices based on Au/PMMA nanocomposites deposited on PEDOT:PSS/Ag nanowire hybrid electrodes," *Appl. Surf. Sci.*, vol. 411, pp. 67–72, 2017.

[17] T. Sannicolo, *et al.*, "Metallic Nanowire-Based Transparent Electrodes for Next Generation Flexible Devices: a Review," *Small*, vol. 12, pp. 6052–6075, 2016.

[18] D.-H. Yoo, *et al.*, "Effect of copper oxide on the resistive switching responses of graphene oxide film," *Curr. Appl. Phys.*, vol. 14, pp. 1301–1303, 2014.

[19] A. Pugliara, *et al.*, "Controlled elaboration of large-area plasmonic substrates by plasma process," *Mater. Res. Express*, vol. 2, p. 065005, 2015.

[20] C. Djaou, *et al.*, "Analysis of the charging kinetics in silver nanoparticles-silica nano-composite dielectrics at different temperatures," *Nano Express*, vol. 2, p. 044001, 2021.

[21] P. Canet, *et. al.*, "Dielectric properties of gold-containing plasma-polymerized thin films," *J. Appl. Phys.*, vol. 72, pp. 2423–2431, 1992.

[22] H. M. Umran, *et al.*, "Ageing: Causes and Effects on the Reliability of Polypropylene Film used for HVDC Capacitor,"*IEEE Access*, vol.8, p.40413-40430, 2020.